ECM2015 | 7th European Combustion Meeting
March 30 – April 2, 2015 Budapest, Hungary

Kinetic processes in complex burning plasma

A.M. Starik

Central Institute of Aviation Motors, Moscow, Russia

Burning plasma

Burning plasma is a multicomponent system involving:

- ✓ Neutral gaseous species
- ✓ Ions and electrons
- ✓ Charged and neutral clusters and particles

Distinctive features of burning plasmas:

- ✓ an absence of external electric field
- ✓ a relatively high temperature (1500-3500 K)
- ✓ a high rate of chemo-ionization reactions
- ✓ an existence of both positively and negatively charged clusters and particles
- ✓ a strong coupling of gaseous and particulate species
- ✓ a broad range of particle sizes (2-100 nm in diameter)

Burning Plasma

Pioneering investigations of electrical properties of hydrocarbon flames were started more than 100 year ago (see, for example, J. Lawton and F. Weinberg, *Electrical Aspects of Combustion*, Oxford University Press (1969); D. K. Bohme, Chemical ionization in flames, *Ion Molecular Reactions*, Plenum Press, New York (1972), p.323–343 ; A. B. Fialkov. *Prog. Energy Combust. Sci., 23, 399–528 (1997).*

Why we need to study processes in burning plasma?

1. **Despite the concentration of ions in flames does not exceed 10^{10}–10^{12} cm^{-3}, i.e. by a factor of 10^8–10^6 smaller than that of neutral molecules, they determine electrical conductivity of flame**
2. **Control of combustion by means of external electric field**
3. **Influence of ions and electrons on the formation of soot particles, fullerenes and nanostructures upon combustion of fuel-enriched hydrocarbon-air mixtures**
4. **Ions can stimulate the formation of condensed phase upon combustion of metalized fuels**
5. **They come into play in the formation of volatile aerosol particles (H_2O/H_2SO_4, H_2O/CH_2O) and contrails in the aircraft exhaust plume**
6. **Diagnostics of combustion processes in the engines of transportation systems by measurements of ionic current**
7. **Plasma-assisted combustion and fuel reforming for gaseous and solid fuels**

Novel challenges and fundamental scientific problems

- **Investigation of cluster and nanoparticle formation in plasma formed during combustion of complex and composite fuels containing metallic particles (Al, Mg, Be etc.) and search the ways to control these processes.**
- **Development of new methods of production of nanostructures with given properties**

Multicomponent plasma including burning plasma is a special interest for researchers in various brunches of science (physics of low-temperature plasma, production of novel materials, physics and chemistry of aerosols, technological processes based on discharge or laser plasma etc.)

This interest is due to special processes taking place in these systems on one side, and vast abilities to obtain structures with unique properties, on the other one.

Sources of ions in the atmosphere

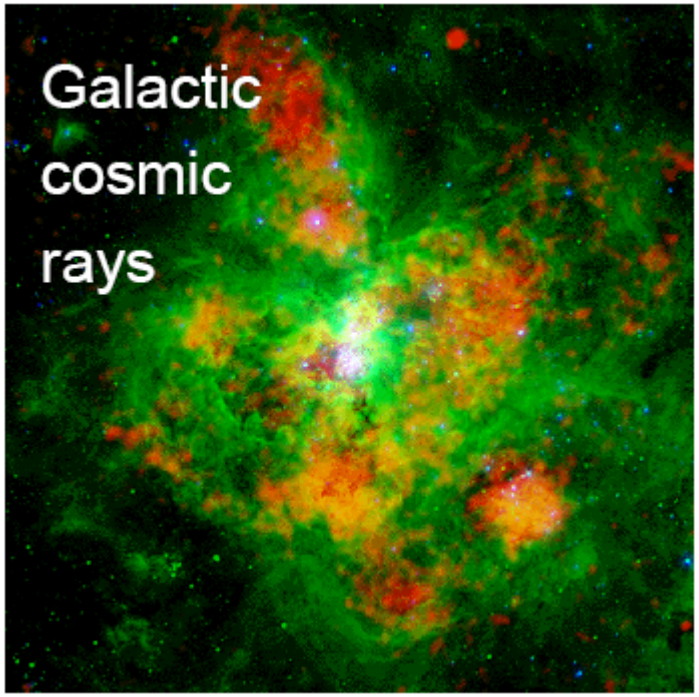

production: <30 ion pairs cm^{-3} s^{-1}
concentration: ~ 2000 ions cm^{-3}
recombination: ~ 350 s

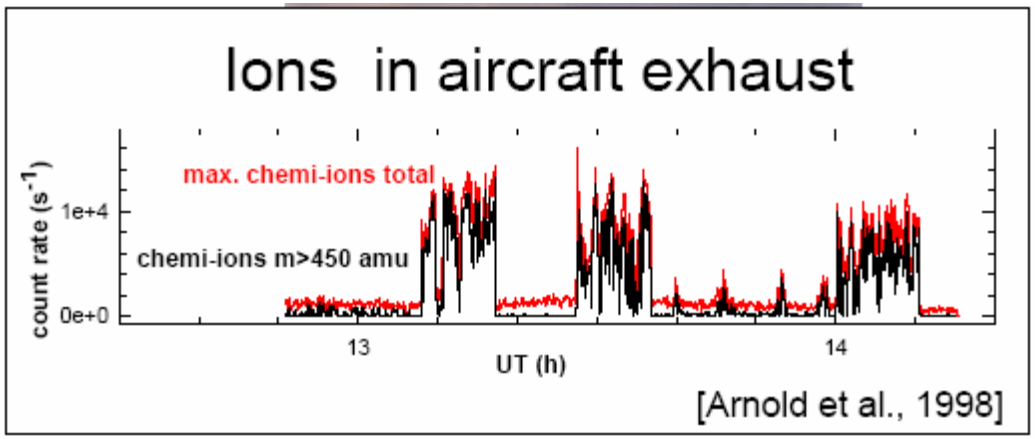

Ions induce the nucleation, condensation growth and contribute to the formation of volatile aerosol particles in the atmosphere

PRINCIPAL SCHEME OF ION FORMATION IN HYDROCARBON+AIR FLAMES

Chemoinization reactions:

$CH+O=HCO^{+}+e$; $N+O=NO^{+}+e$

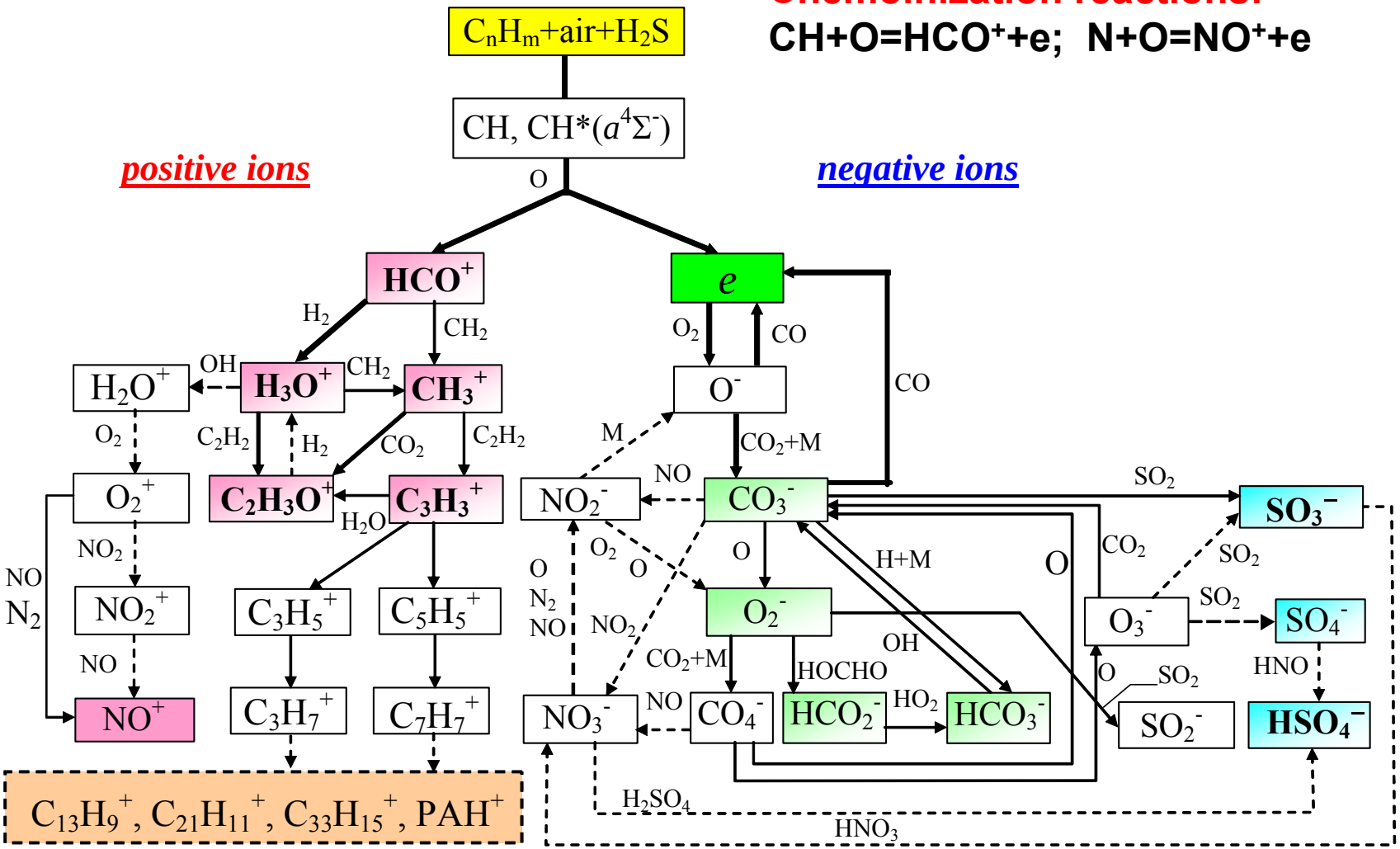

Reactions of chemi-ions formation involved in kinetic model

Type of reaction	Symbols	Reactions products
1. Reaction with CH, CH($a^4\Sigma^-$)	$CH(CH^*)+O=HCO^++e^-$ $CH^*+C_2H_2=C_3H_3^++e^-$ $N+O=NO^++e$	HCO^+, $C_3H_3^+$, e^-
2. Associative ionization	$A+B=AB^++e^-$	N_2^+, O_2^+, NO^+, $C_3H_3^+$, e^-
3. Dissociative ionization	$AB+e^-=A^-+B$	O^-, O_2^-, NO_2^-
4. Ionization under molecule and electron interaction	$AB+e^-=AB^++2e^-$	O_2^+, N_2^+, NO^+, O^+, N^+
5. Associative electron attachment	$AB+e^-=AB^-$	O^-, O_2^-, NO^-, NO_2^-
6. Nonresonance charge exchange	$A^++B=A+B^+$	N_2^+, N^+, O_2^+, O^+, NO^+, NO_2^+, NH_3^+, CO^+, CO_2^+
	$A^-+B=A+B^-$	NO_2^-, NO_3^-, O^-, O_2^-, O_3^-, H^-, OH^-, SO_2^-
7. Binary ion-molecular reactions	$A^++BC=B+AC^+$	HCO^+, H_3O^+, CH_2OH^+, H_2O^+, CH_3^+, $C_2H_3O^+$, $C_2H_3^+$, $C_3H_3^+$, C^+, N_2^+, N^+, NO^+, NO_2^+, NH_3^+, NH_4^+, O^+, O_2^+, CO^+, $C_3H_5O^+$, $C_3H_7O^+$
	$A^-+BC=B+AC^-$	NO^-, NO_2^-, NO_3^-, O^-, O_2^-, O_3^-, O_4^-, OH^-, CN^-, CO_3^-, CO_4^-, SO_2^-, SO_3^-, SO_4^-, HSO_4^-, $HCOO^-$, HCO_3^-
8. Ion-molecular reactions with electron formation	$AB^-+C=e^-+A+BC$	e^-
9. Ternary recombination of ion and neutral	$A^++B+M=AB^++M$	N_2^+, NO^+, O_2^+
10. Dissociative recombination	$A^-+B+M=AB^-+M$	NO_2^-, O_3^-, CO_3^-, O_4^-, O^-, CO_4^-, HCO_3^-
	$AB^++e^-=A+B$	Neutral
11. Ion-electron recombination	$AB^++e^-=AB$	Neutral
12. Binary ion-ion recombination	$AB^-+C^+=AB+C$	Neutral
13. Ternary ion-ion recombination	$AB^-+C^++M=AB+C+M$	Neutral

Kinetic model of hydrocarbon fuel combustion

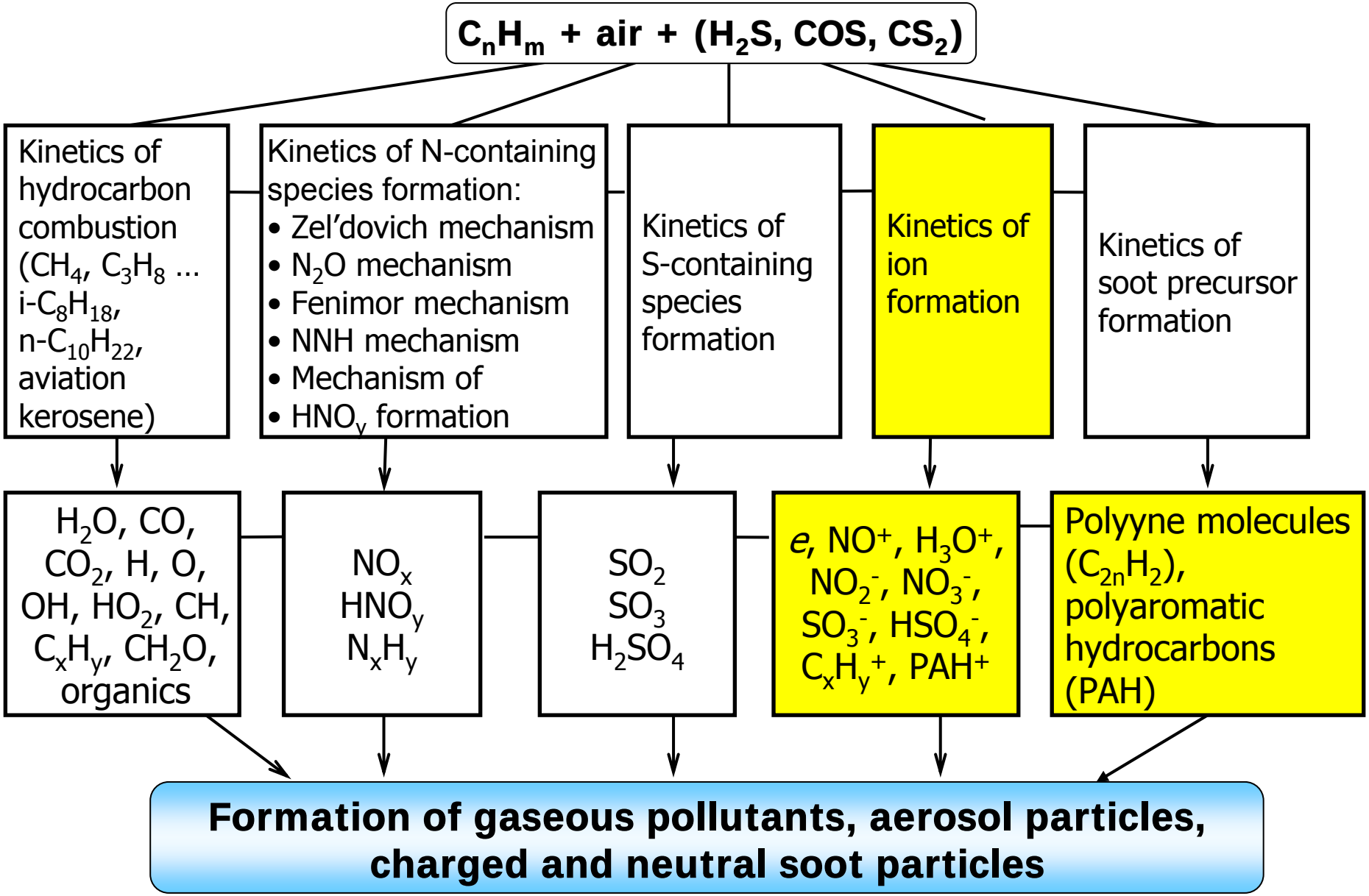

Ion formation in flames

Model (Rodrigues, PSST. 2007)

- ✓Temperature profile was calculated using PREMIX code from CHEMKIN software package
- ✓The computed temperature profile was used for modeling of charged species evolution in flame with detailed ion kinetics
- ✓The diffusion of ions was ignored
- ✓Reaction mechanisms involves more than 1300 reversible reactions with neutral and charged species

C_3H_8 + air

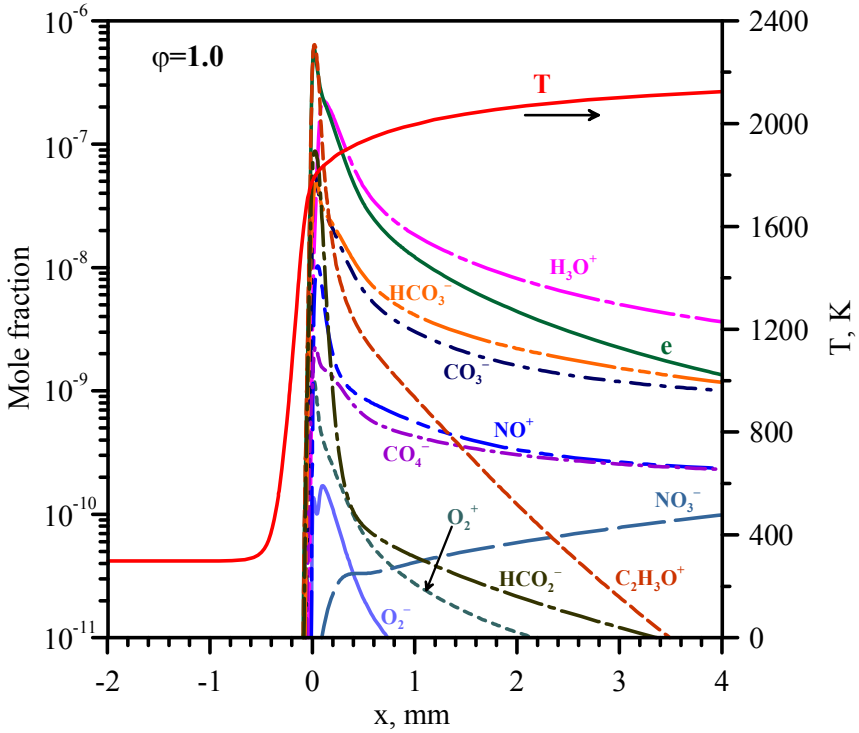

Predicted spatial profiles of ion mole fractions and temperature in stoichiometric propane/air atmospheric pressure flame.

Kinetic models: ***CH_4-air*** – Starik A.M.,Titova N.S. Combust. Explos.Shock Waves.2002; Prager J.et al. *PROCI.**2007.***
C_3H_8-air - Rodrigues J.M. et al. P*lasma Sources Sci. Technol.* ***2007.***

The most abundant ions:
in the flame front - **$C_2H_3O^+$, HCO_2^-** ions and **electrons**;
behind the flame front - **H_3O^+** ions and **electrons**.

Ion formation in flames

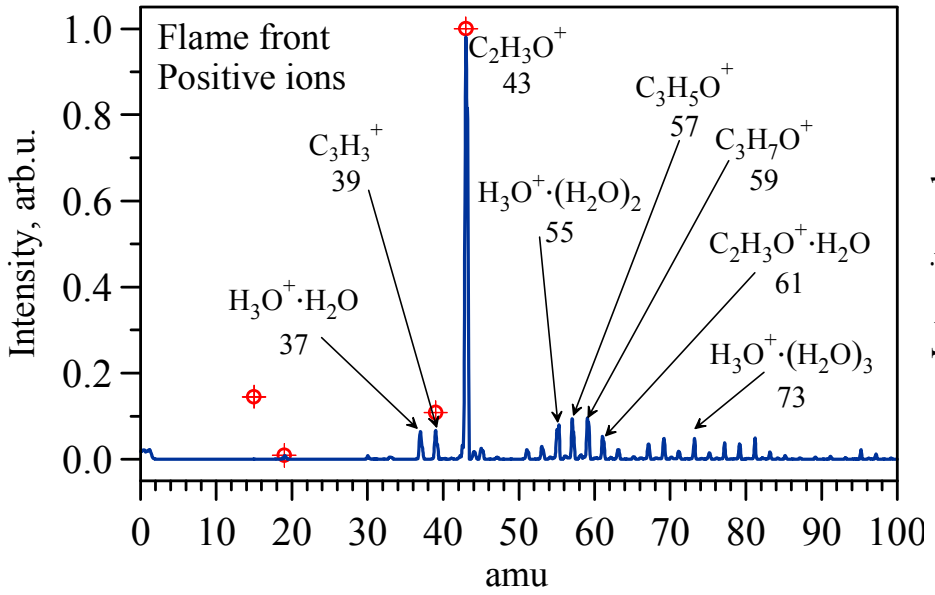

Positive ions

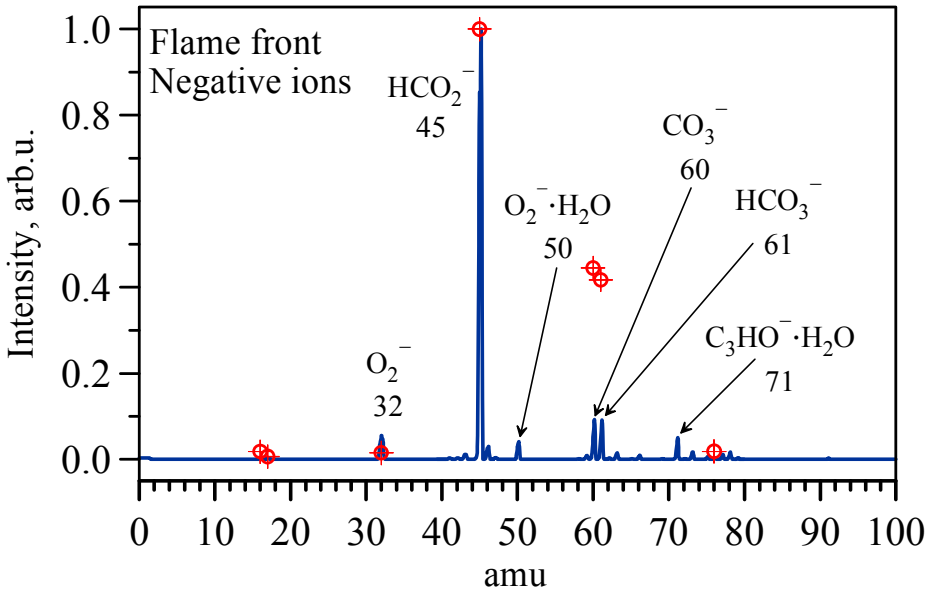

Negative ions

Observed and predicted mass-spectra of positive and negative ions normalized on ion with maximal concentration in the flame front of stoichiometric atmospheric propane/air flame (*J.M. Rodrigies et al. PSST, 2007*). Symbols are predictions.

The computed ion concentrations are in reasonable agreement with experimental data.

Why ionic clusters $H_3O^+(H_2O)_n$ were detected in the flame front? Are they actually abundant in flame?

Scheme of mass-spectrometer extraction system

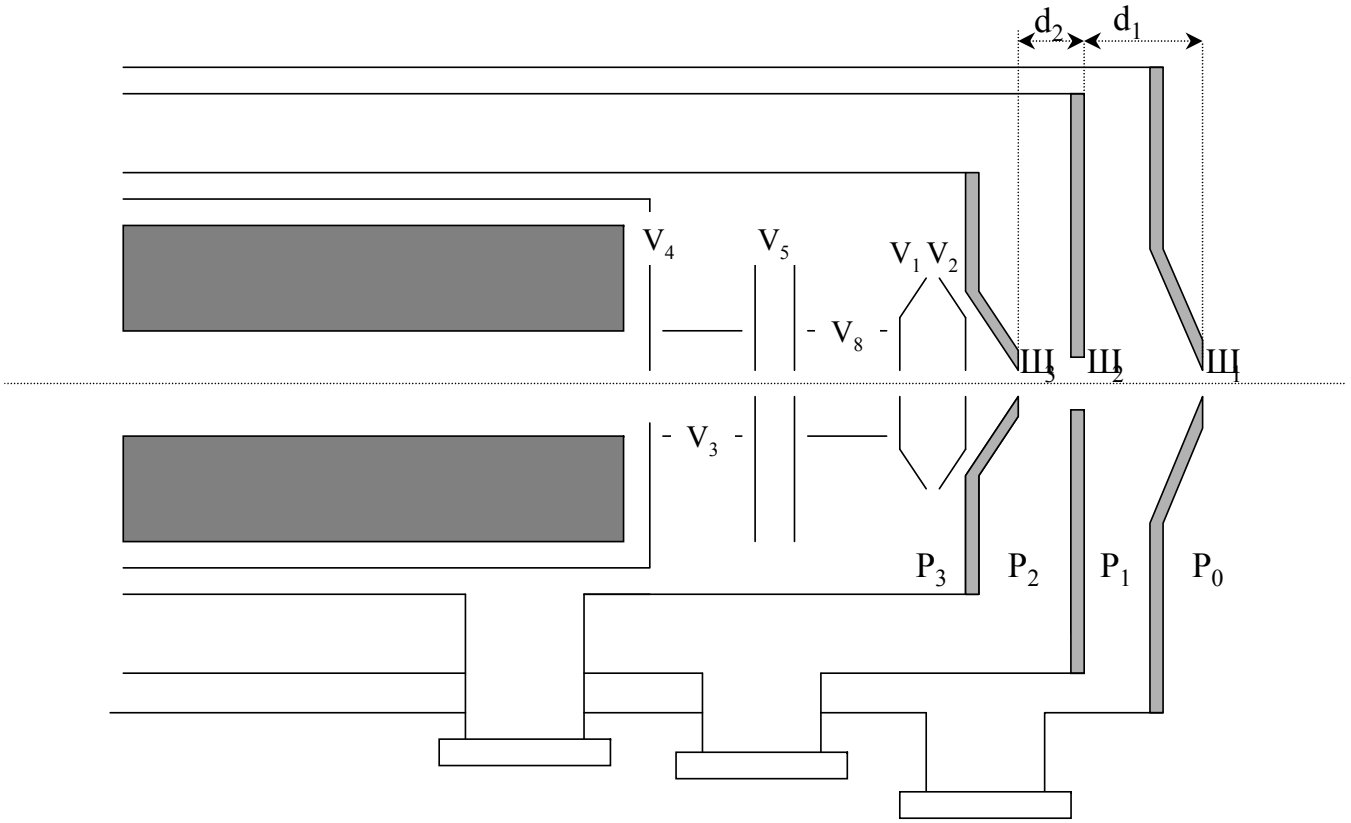

P_0=760 torr

P_1=5.10^{-3} torr

P_2=10^{-3} torr

P_3=5.10^{-6} torr

$\varnothing_1$=0.1mm

$\varnothing_2$=0.5mm

$\varnothing_3$=0.1mm

d_1=18mm

d_2=15mm

Volts	V_1	V_2	V_3	V_4	V_5	V_6	V_7	V_8
Positive ions	0	0	30	25	60	300	140	125
Negative ions	0	0	-30	-25	-65	-300	-120	-125

Ion transformation in mass spectrometer channel

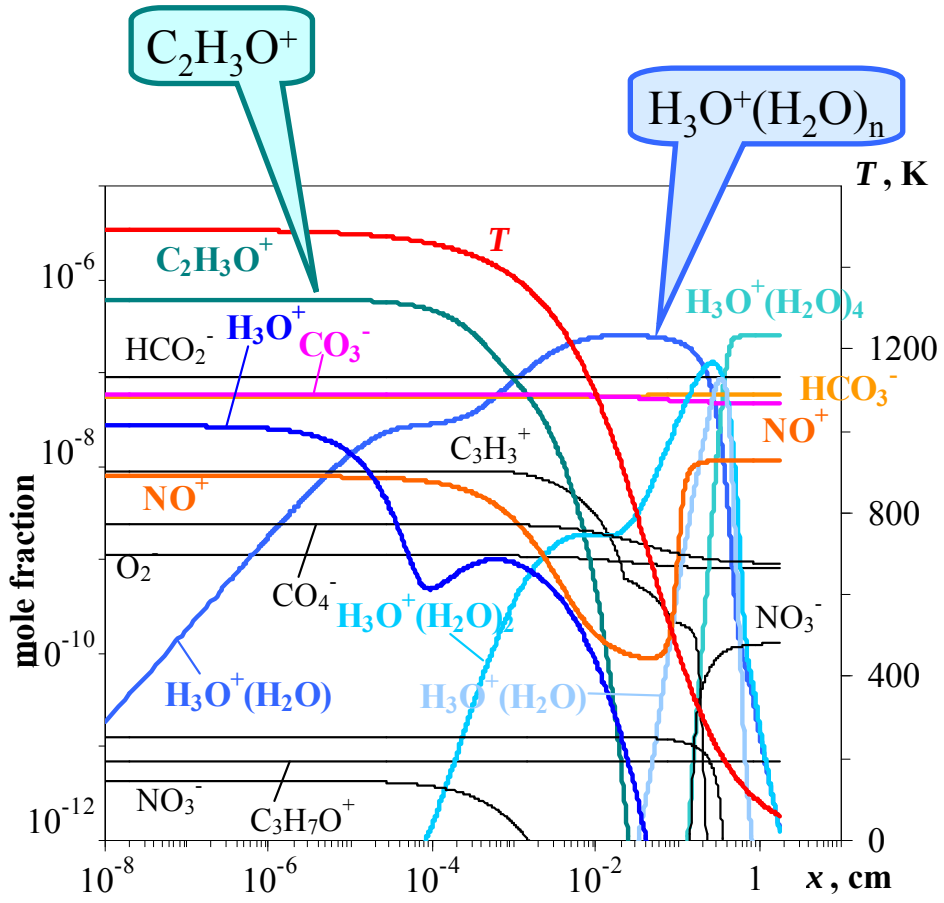

Evolution of temperature and ion mole fractions along the extraction system of mass spectrometer channel

We supposed that in the flame there are no ionic clusters $H_3O^+(H_2O)_n$ and only H_3O^+ ions are abundant!

1. Concentration of positive hydrocarbon ions $C_2H_3O^+$ decreases at a short distance inside the mass spectrometer channel and $C_2H_3O^+H_2O$ form
2. The ionic clusters $H_3O^+(H_2O)_n$ form in a large amount inside the mass spectrometer. **Such clusters do not form in the flame.**

Ion formation in flames

During combustion of complex hydrocarbon fuels, for example, aviation kerosene containing sulphur in a trace amount, the S-containing species form and such ions as SO_4^-, SO_3^-, HSO_4^- arise.

Distinctive feature of diffusion fluxes for the charged species is the necessity of allowing for the diffusion caused not only the concentration and temperature gradient but also owing to the appearance of internal electric field due to diffusion separation of ions and electrons (ambipolar diffusion).

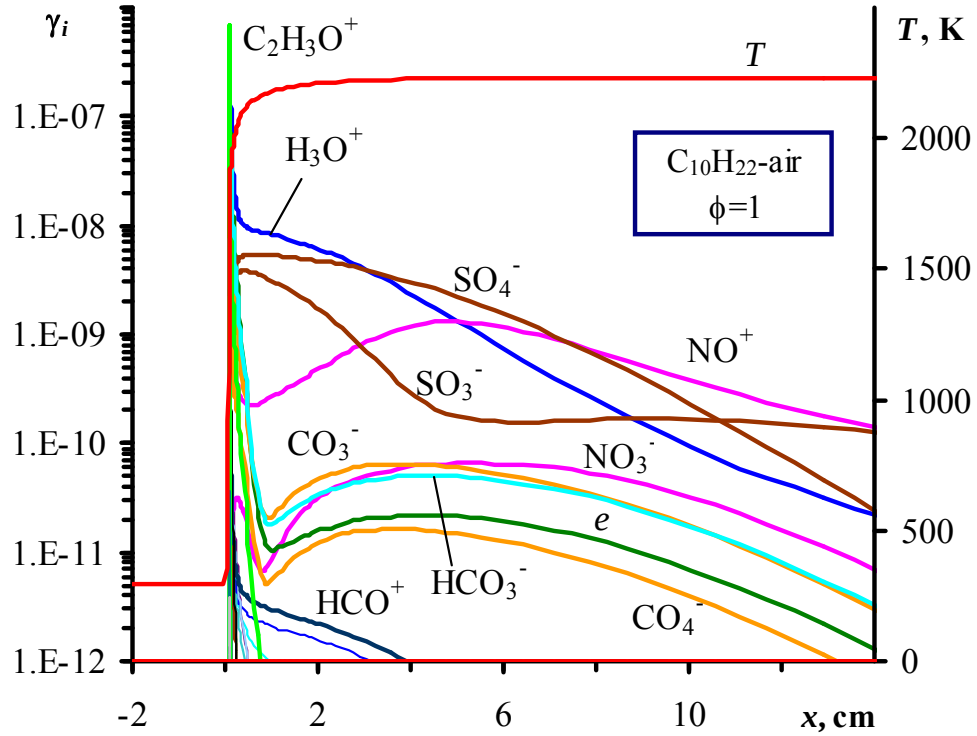

Predicted spatial profile of ion mole fractions and temperature in atmospheric pressure flame for surrogate fuel **decane / H_2S** representing the aviation kerosene with 0.04% fuel sulfur content.

The most abundant ions: in the flame front - **$C_2H_3O^+$, HCO_3^-** and **electrons**;
behind the flame front - **H_3O^+, NO^+, SO_4^-,** and **SO_3^-**;
at the large distance from the flame front - **NO^+** and **SO_3^-**

Charged soot particle formation

Basic mechanisms

1. Chemical condensation of heavy hydrocarbon ions: $C_{13}H_9^+$, $C_{21}H_{11}^+$, $C_{33}H_{16}^+$, $C_{45}H_{17}^+$ and others (soot precursors) $\Rightarrow$ the formation of positively charged soot particles in the fuel rich zone (*Calcote and Keil, Pure Appl. Chem, 1990*; *Weilmuster P. et al. Combust. Flame, 1999*)
2. Thermal ionization of soot particles: $p^{q-1} \rightarrow p^q + e^-$ $\Rightarrow$ positively charged particles at initial stage $\Rightarrow$ ion formation $\Rightarrow$ ion/electron attachment to particles (*Balthasar et al. Combust. Flame, 2002*)
3. Formation of positively and negatively ions and electrons via chemo-ionization and plasma chemical reactions $\Rightarrow$ charging of clusters and soot particles (*Savel'ev and Starik, Technical. Phys. 2006*)

Positive chemi-ions: NO^+, H_3O^+, $C_nH_mO^+$, $C_nH_m^+$
Negative chemi-ions: HCO_2^-, HCO_3^-, NO_3^-, NO_2^-, HSO_4^-, SO_3^-,O_2^-, O^-, CO_3^-, CO_4^-, electrons

* **Onischuk et al. (*Aerosol Science. 2003*) observed positively and negatively large size particle (d>50 nm) with q=±(5-10)e in diffusion propane/air flame**
* **Maricq (*Combust. Flame 2005, 2006*) detected the symmetrical charge distribution of small and middle size particles (d=13 and 34 nm) in C_2H_4/air, C_2H_6/air, and C_2H_2/air flames.**

Soot particle formation

- ✓Soot particles are believed to form from polyyne molecules and polyaromatic hydrocarbon (PAH) molecules. Pyrene $C_{16}H_{10}$ molecules (with diameter d_p=0.724 nm) which consist of four benzene rings are considered as the main soot precursor. The concentration of pyrene in the fuel rich zone of combustor can be as large as 10^{12}-10^{14} cm^{-3}.
- ✓The primary clusters with d=2 nm that serve as the inception particles are constructed from PAH via PAH-PAH coalescence. The concentration of primary cluster mounts to 10^{11}-10^{12} cm^{-3}.
- ✓Surface growth and surface oxidation
- ✓Attachment of ions and electrons to particles
- ✓Coagulation of neutral and charged particles
- ✓Thermoemission

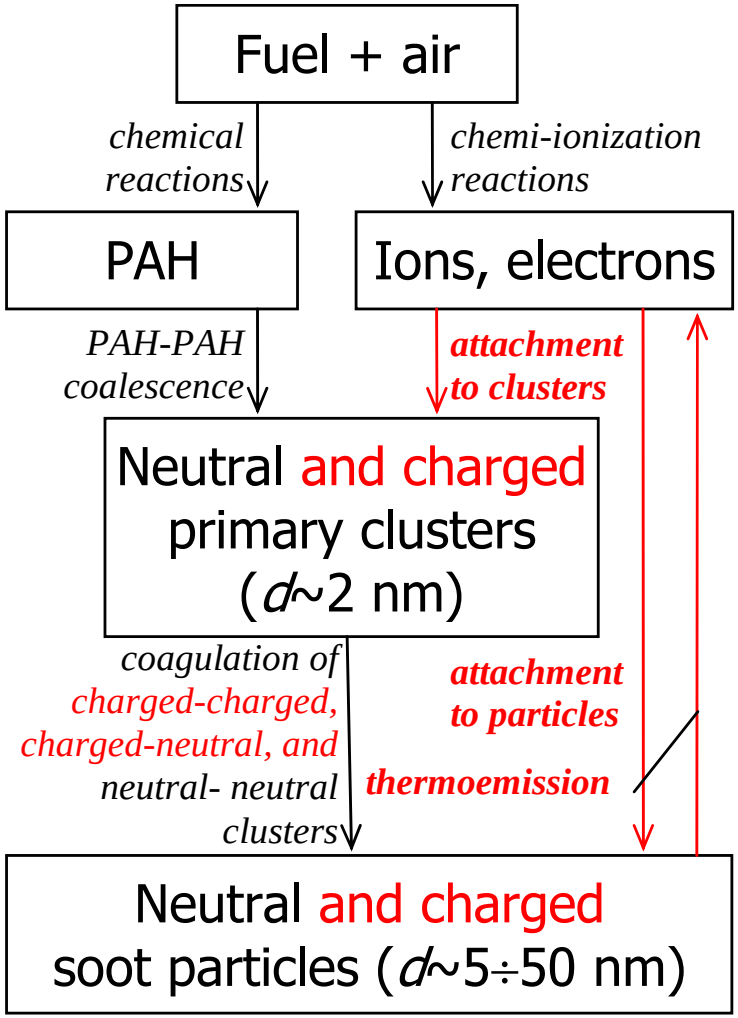

Model description:

1. Starik A.M. et al. Plasma Sources Sci. Technol. 2008. V.17/17/4/045012.
2. Savel'ev A.M. et al. Doclady Physics. 2008. V.53. No.6. 312-317.
3. Savel'ev A.M. and Starik A.M. JETP. 2009. V.108. No.2. 326-339.

Ion-Particle Interaction

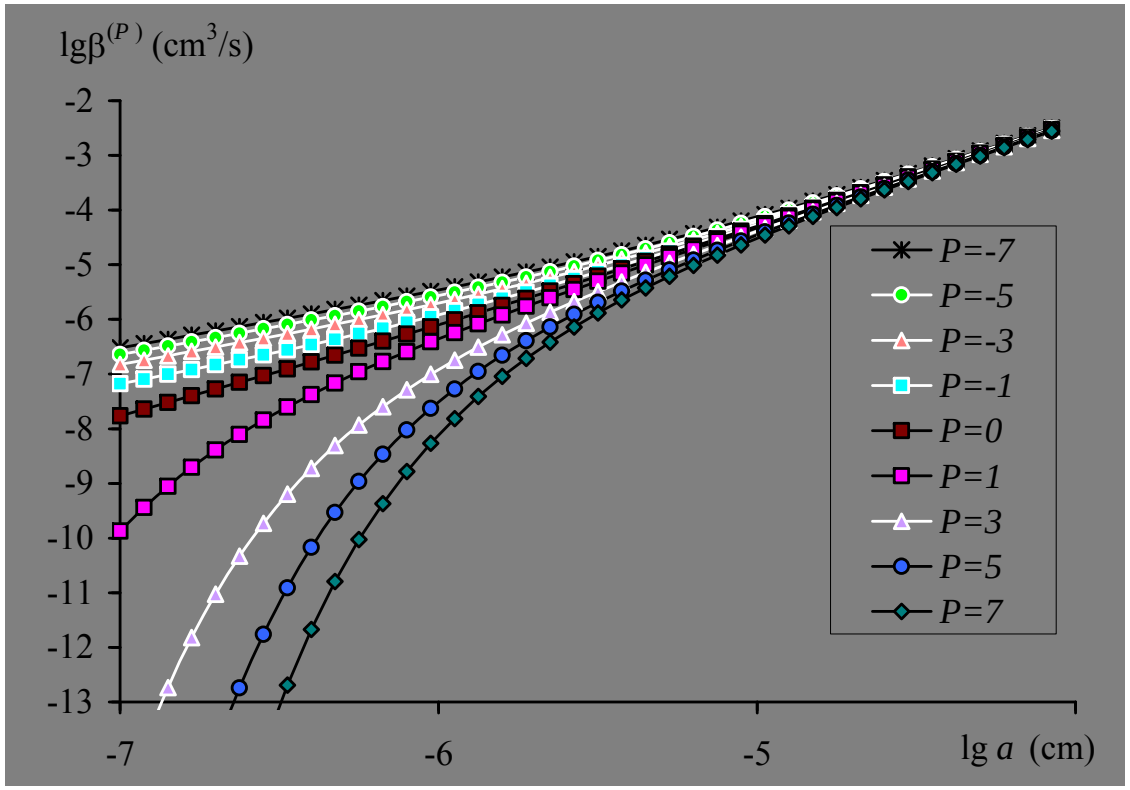

Attachment coefficient, $\beta^{(p)}$, for NO^+ ion to soot particle with different charge p = -7, …, +7 ($p=q_i \cdot q_n$) as a function of particle radius, a.

Coulomb and electric image forces

$$\varphi(r) = \frac{pe^2}{r} - \frac{e^2 a^3}{2r^2\left(r^2 - a^2\right)}$$

$$\Rightarrow \sigma(V) = f(a, p, m, T)$$

$$\beta^{(p)} = \langle V\sigma \rangle = \int \sigma(V)\, V\, f_m(V) dV$$

Parameters:
T=2000 K, P=10^5 Pa,
a=1-50 nm,
free length $\lambda(NO^+)$=150 nm

Ions and particles with the same polarities can attract. At T ~ 2000 K the probability for even small particles with $a \geq 5$ nm to accumulate a few elementary charges is rather large.

Charged soot particle formation

Mathematical Model

$$\frac{\partial P_q}{\partial t} + \nabla\left(P_q V\right) = W_{at} + W_c + W_{th}$$

$$W_{at} = P_{q-1}\sum_{i=1}^{N_1} n_i^+ \beta^+\left(m, q-1, \mu_i^+\right) + P_{q+1}\sum_{j=1}^{N_2} n_j^- \beta^-\left(m, q+1, \mu_i^-\right)$$

$$W_c = \sum_{q_1=-\infty}^{\infty} \nu\left(x, q-q_1\right)\int_0^{\infty}\int_0^{\infty} P_{q_1}\left(m_1\right)P_{q_1-1}\left(m_2\right)\kappa\left(q_1, q-q_1, m_1, m_2\right)\delta\left(m-m_1-m_2\right)dm_1 dm_2 -$$

$$- P_q(m)\sum_{q_1=-\infty}^{\infty}\int_0^{\infty} P_{q_1}\left(m_1\right)\kappa\left(q_1, q, m_1, m\right)dm_1$$

$$\nu\left(q_1, q-q_1\right) = \begin{cases} \frac{1}{2}, & x = q-q_1 \\ 1, & x \neq q-q_1 \end{cases}$$

$$W_{th} = P_{q-1}h\left(a(m), q-1\right) - P_q h\left(a(m), q\right)$$

$$h\left(a(m)\right) = 4\pi a^2 A T^2 \exp\left(-\frac{\varphi_w}{kT}\right) \qquad q < 0$$

$$h\left(a(m), q\right) = 4\pi a^2 A T^2\left(1 + \frac{(q+1)e^2}{4\pi\varepsilon_0 akT}\right)\exp\left(-\frac{1}{kT}\left\{\varphi_w + \frac{(q+1)e^2}{4\pi\varepsilon_0 a}\right\}\right) \qquad q > 0$$

To integrate numerically the kinetic equations the Euler's method of fractions was used.

$P_q(m)dm$ is the concentration of particles with charge q and with the mass being in the range from m to $m+dm$

φ_w is the work function

The φ_w value was assumed to be equal that for graphite.

Particle coagulation

The mechanisms of cluster and particle interaction

- **Coulomb force**
- **Van-der-Waals force**
- **Image force**

$d = 2 - 100$ nm

- The forces caused by transferring pulse by ions to interacting particles can be significant only for micrometer size particles ($d > 5$ μm)

Saveliev A.M., Starik A.M. //JETP. 2009.

Particle coagulation

Effective potential

$\Phi(r)=\Phi_m(r)+\Phi_e(r)$

$\Phi_e(r)=\Phi_c(r)+\Phi_{im}(r)$ $\quad x=(R_1+R_2)/r,\ s=R_1/(R_1+R_2)$

Van-der-Waals potential

$$\Phi_m(x)=-\frac{\overline{H}}{6}\left(\frac{2s(1-s)x^2}{1-x^2}+\frac{2s(1-s)x^2}{1-(2s-1)^2x^2}+\ln\left(\frac{1-x^2}{1-(2s-1)^2x^2}\right)\right)$$

For charged-charged particles

$$\Phi_e(x)=\Phi_c(x)-M\frac{px}{2}\left(\frac{z_1^2s^3x^3}{1-s^2x^2}+\frac{z_2^2(1-s)^3x^3}{1-(1-s)^2x^2}\right)$$

Coagulation of particles due to exerting of Van- der-Vaals force

Potential of interaction

$$\hat{\Phi}(x) = -\frac{\hat{H}}{6}\left(\frac{2s(1-s)x^2}{1-x^2} + \frac{2s(1-s)x^2}{1-(2s-1)^2x^2} + \ln\left(\frac{1-x^2}{1-(2s-1)^2x^2}\right)\right),$$

$$x = (R_1 + R_2)/r, \quad s = R_1/(R_1 + R_2)$$

Coagulation rate constant

$$K = \frac{1}{2}\pi\langle V\rangle(R_1 + R_2)^2\,\beta_{dd},$$

$$\beta_{dd} = \int_0^1 \frac{1}{\gamma}\left\{\frac{1}{\gamma}\frac{d\hat{\Phi}(\gamma)}{d\gamma} - \frac{d^2\hat{\Phi}(\gamma)}{d\gamma^2}\right\}\exp\left(\frac{\gamma}{2}\frac{d\hat{\Phi}(\gamma)}{d\gamma} - \hat{\Phi}(\gamma)\right)d\gamma.$$

R_1, R_2 are the radii of particles, $\hat{H} = H/k_B T$ Is the dimensionless Hamaker constant,

$\langle V\rangle$ is the mean velocity of relative particle motion, $\gamma=(R_1 + R_2)/\delta$, δ – radius of capture sphere,

H = 6.4×10-20 J. ***Chan et al. // J. Aerosol Sci. 2001***

Saveliev A.M., Starik A.M. //JETP. 2009.

Coagulation for charged and neutral particles

Enhancement factor for coagulation rate due to exerting of image force between primary charged and neutral particles and between two charged particles as a function of particle radius, a_2. Parameters T=2000 K, P=10^5 Pa.

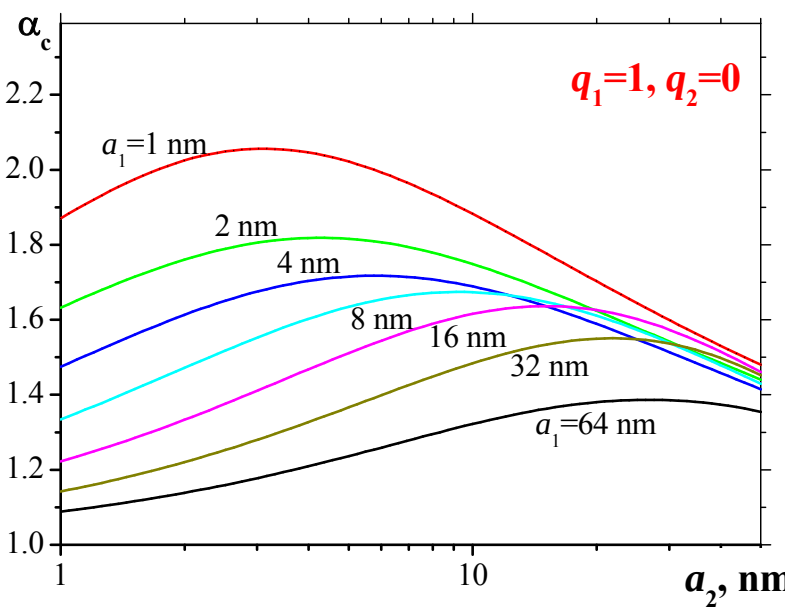

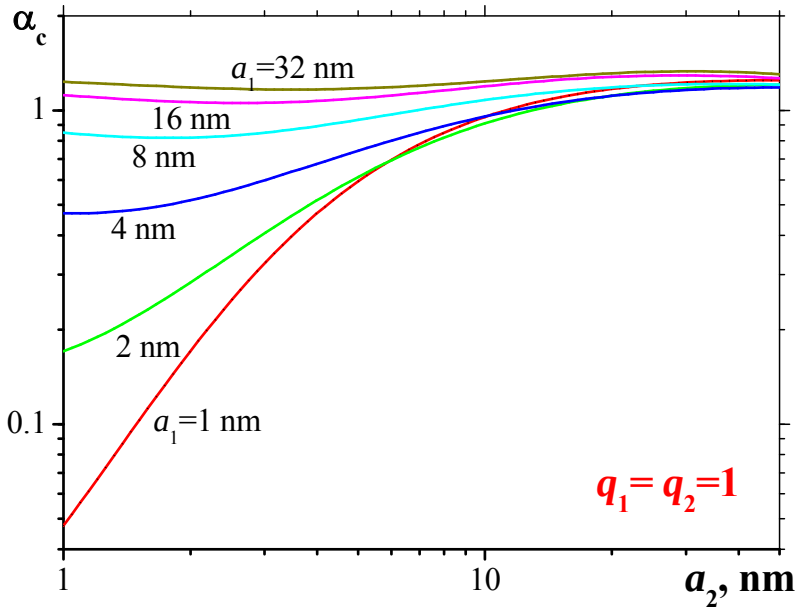

Even at high temperature (T~2000 K) the exerting of image force can increase the coagulation rate for single charged and neutral particles interaction up to a factor of 2, for larger charge of the particle (q_1=3e) the enhancement factor may be a large as 4. The presence of the polarization force leads to a situation when even two particles with identical charges can coagulate with a rate that is greater than its gas kinetic value, even despite the Coulomb repulsion.

COAGULATION OF CHARGED CLUSTERS

Assumptions: (1) there exists monodispers distribution of primary clusters, r_0=1 nm; (2) concentration of this clusters is 10^{11} cm^{-3}; (3) conditions correspond to the combustion of fuel rich n-$C_{10}H_{22}$+air mixture, ϕ=3: T_c=2050 K, P_c=0.1 MPa

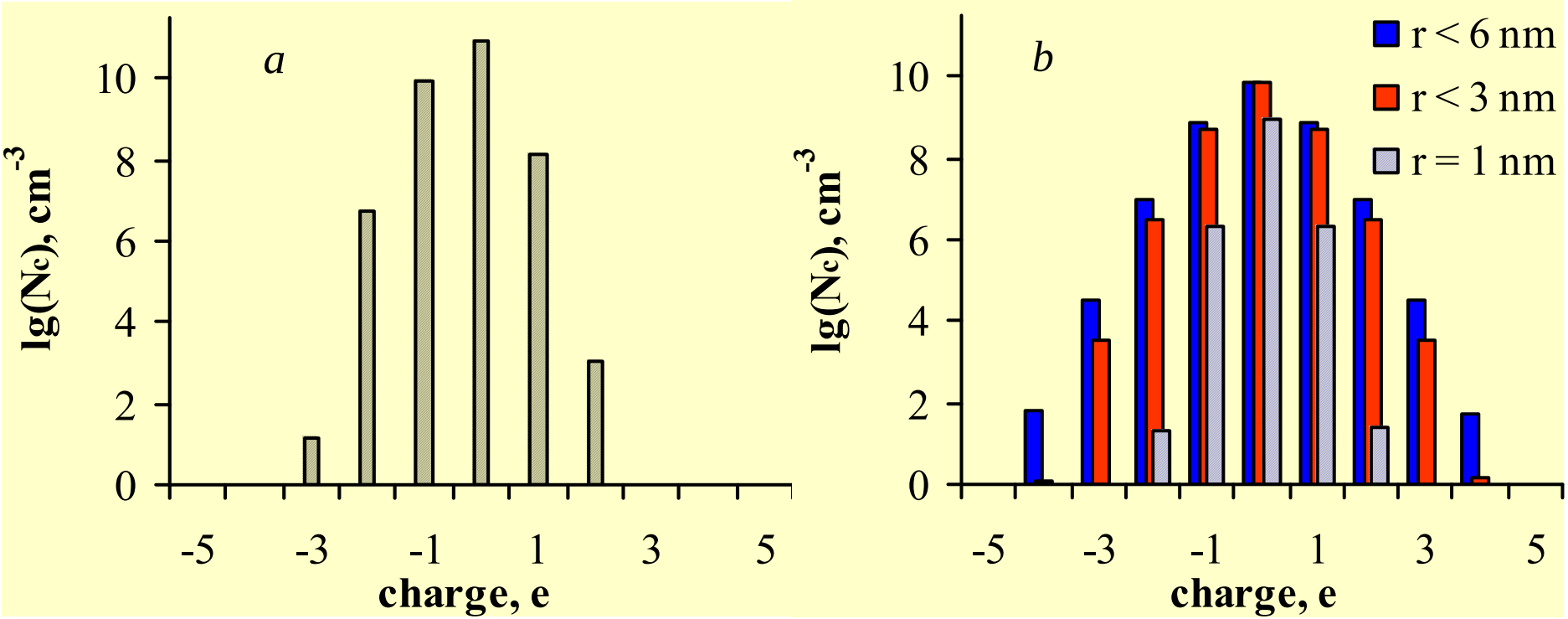

Charge distribution of clusters with radius smaller than given value at $N_0=10^{11}$ cm^{-3}, r_0=1 nm for the conditions corresponding to the fuel rich region of combustor at time instants of 0.1 ms and 5 ms.

Charging of primary clusters accelerates the coagulation process considerably both due to charged-charged and charged-neutral cluster interaction

Kinetic processes in combustion complex plasma

Ion-particle interaction + coagulation (without thermal ionization)

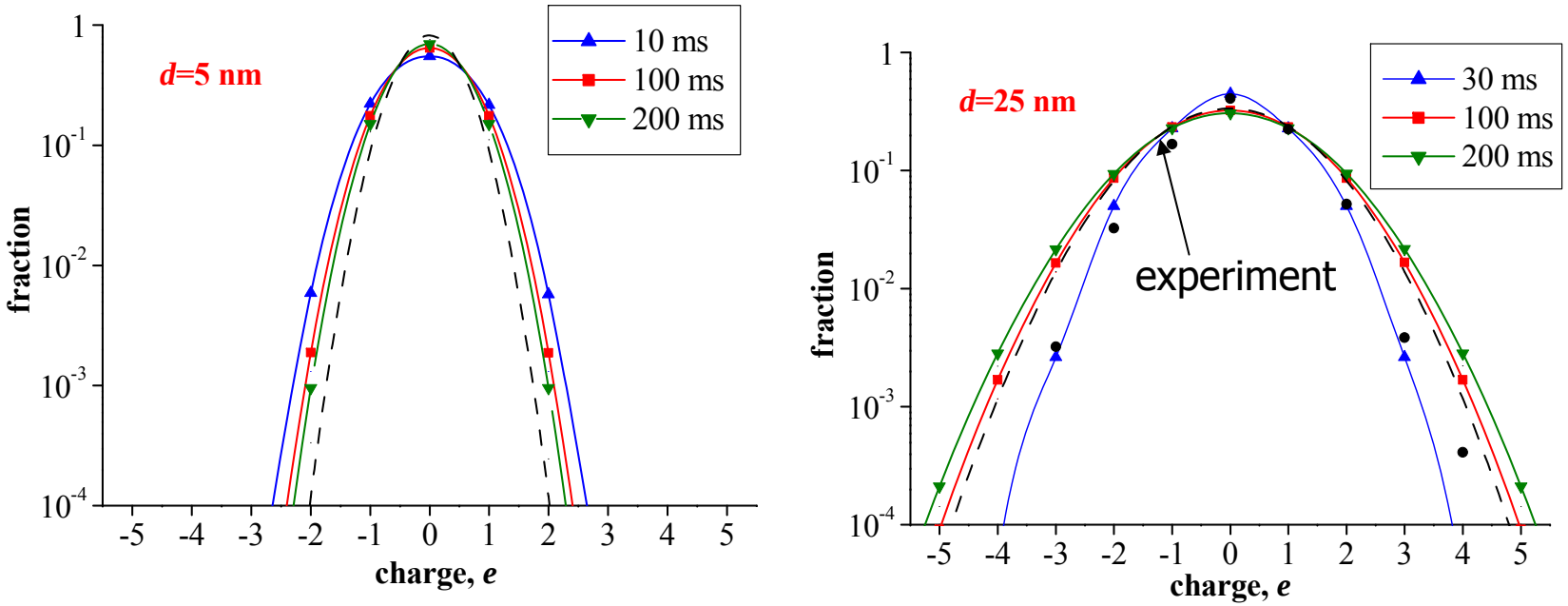

Predicted and measured charge distribution of soot particles for C_2H_4-air flame with ϕ=2.04 (Maricq C&F. 2005) at different time instants in the case when thermal emission is excluded from the model.

- ✓ Ion-particle interaction and coagulation of the particles make it possible to predict with rather high accuracy the measured symmetrical charge distribution behind the flame front.
- ✓ For small size particles (d<10 nm) the Boltzmann charge distribution is not achieved. For large particles (d>25 nm) the charge distribution is close to Boltzmann one.
- ✓ The calculated charge distribution of particles at t=30 ms is in a good agreement with the experimental data (*Maricq, Comb. Flame, 2005*).

Kinetic processes in combustion dusty plasmas

Effect of ion-particle interaction

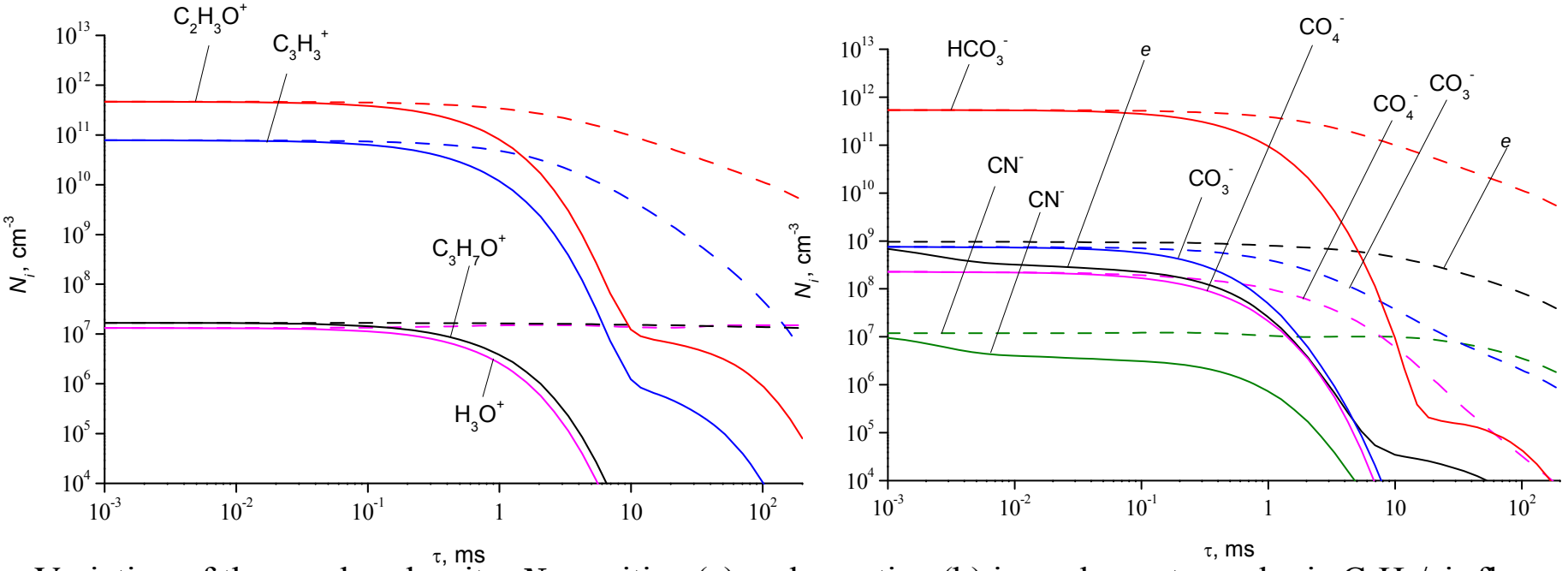

Variation of the number density, N_i, positive (a) and negative (b) ions along atmospheric C_2H_4/air flame (ϕ=2.06) with ion-particle interaction (solid curves) and without such interaction (dashed curves).

Ion-particle interaction considerably affects the change in ion and electron concentrations. The decrease in ion number density is associated with attachment of ions to particles. That is why Calcote and Keil (1990) observed the strong decrease in ion number density after starting soot particle formation.

Ion formation in aviation combustor

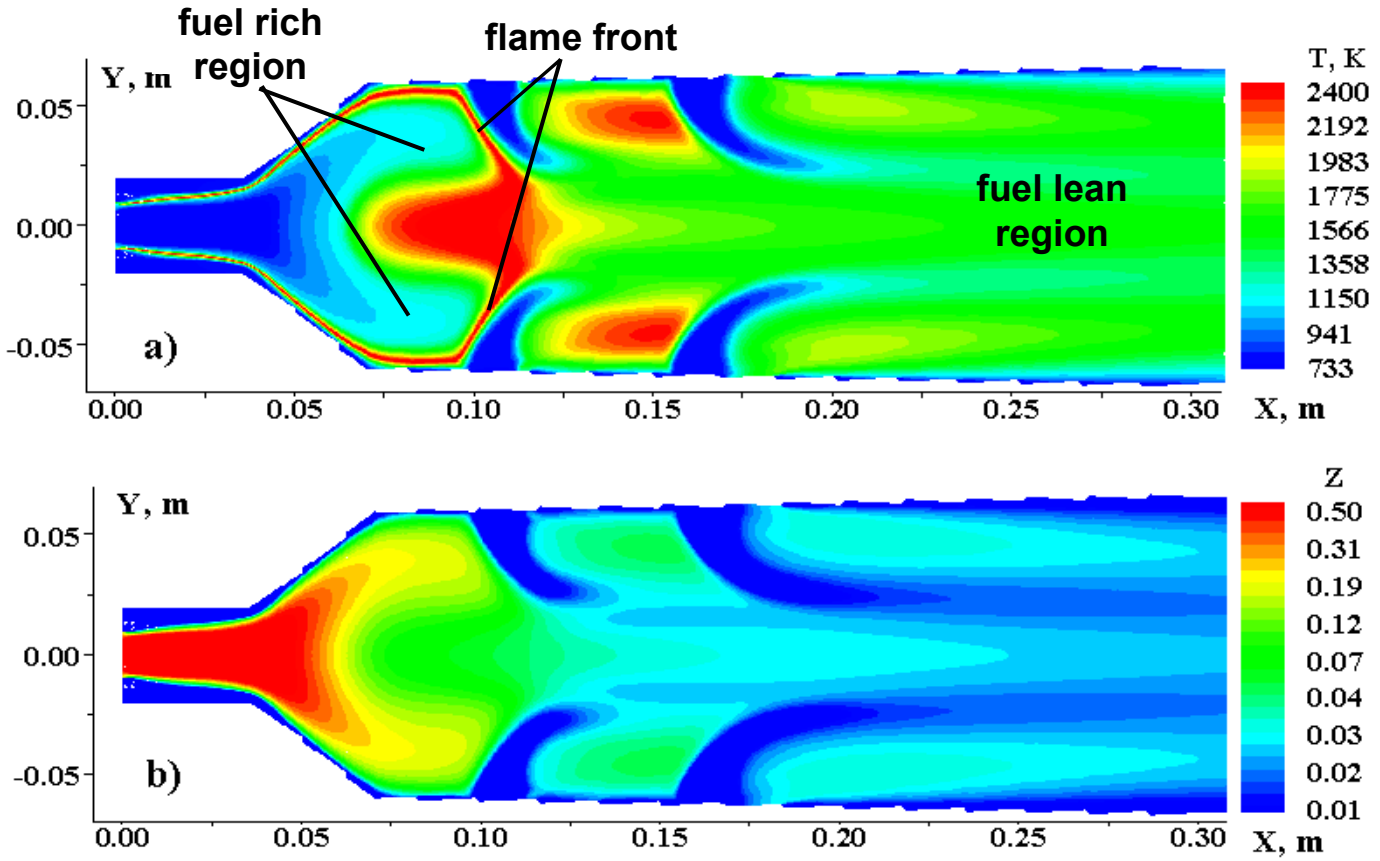

The temperature (a) and mixture fraction (b) fields inside the combustor that is close to those of PC-90 bypass engine.

Parameters: P=1.16 MPa, T_{air}=733 K, methane/air equivalence ratio ϕ=0.33, mixture fraction Z=1(1+ S/ϕ), S is the stoichiometric coefficient, STAR-CD + post processor for ions.

Ion formation in aviation combustor

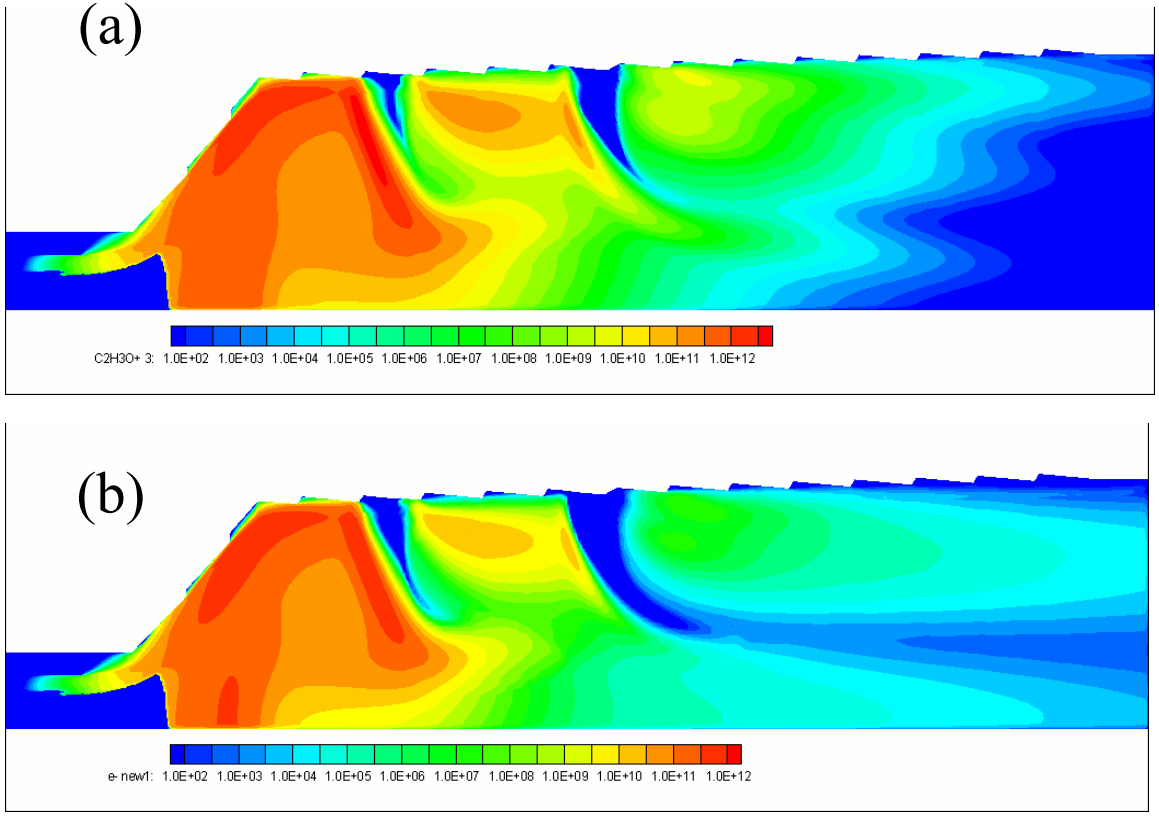

- **Maximal concentration of charge species in the fuel rich zone of combustor is found for $C_2H_3O^+$ ions and electrons.**

$N_{ion} \sim 10^{12}$ cm^{-3}

The $C_2H_3O^+$ ion (a) and electron (b) mole fraction fields in aviation combustor under combustion of CH_4/air mixture (STAR-CD + Flame Let Model).

Ion formation in aviation combustor

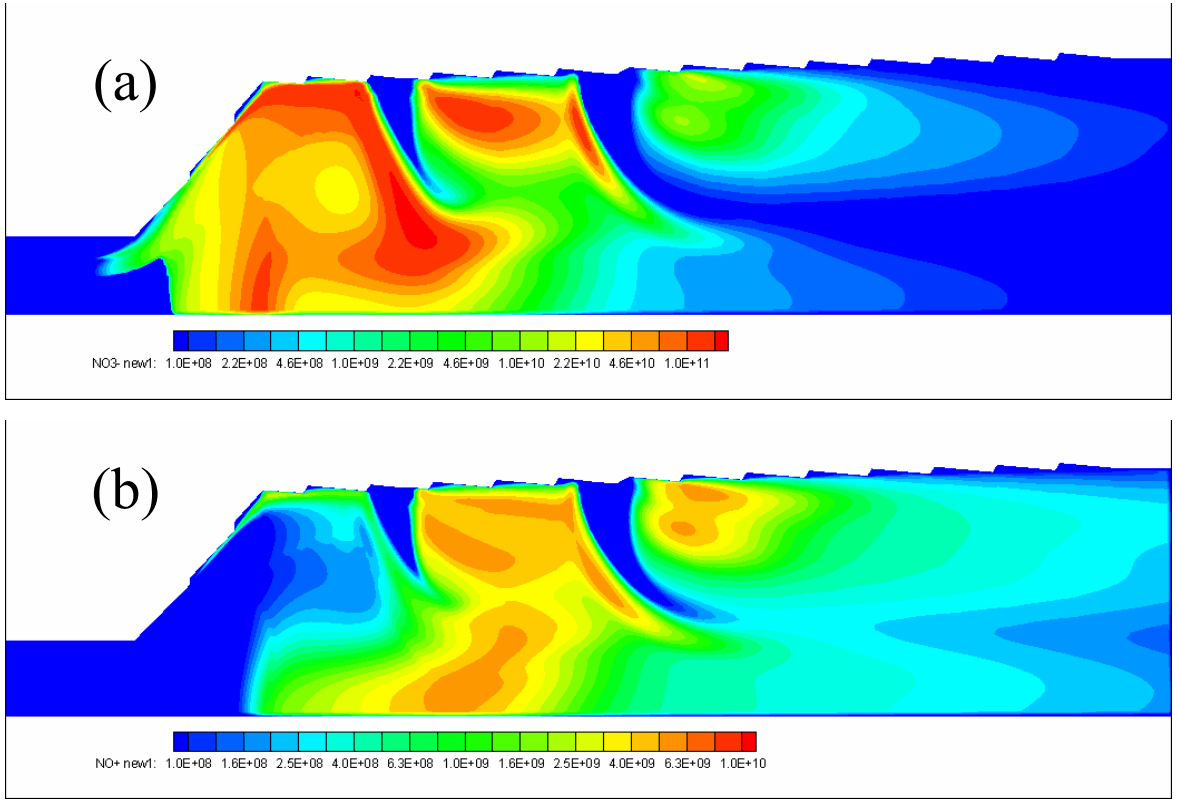

- Maximal concentration of charge species in **the combustor exit is found for NO^+ and NO_3^- ions.**

$N_{ion} \sim 2 \cdot 10^8$ cm^{-3}

The NO_3^- (a) and NO^+ (b) ion mole fraction fields in aviation combustor under combustion of CH_4/air mixture (STAR-CD + Flame Let Model).

- **The computed ion concentration at the combustor exit ($2 \cdot 10^8$ cm^{-3}) is in a good agreement with measurements of Arnold F. et. al.** (*Haverkamp H., Wilhelm S., Sorokin A., and Arnold F., Atmospheric Environment, 2004*).

Acquisition of polar molecules by charged soot particles in combustor

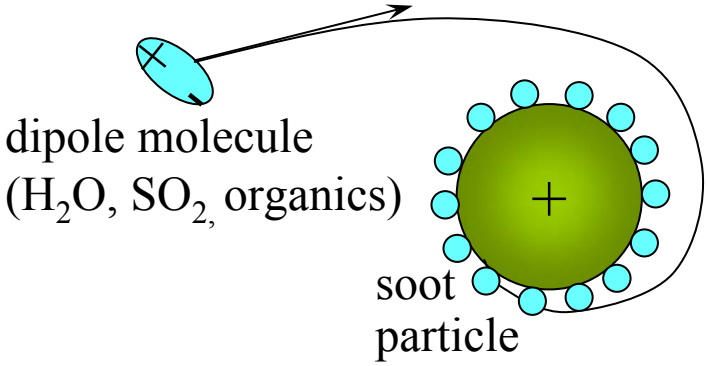

Fuchs theory (1964)

$$\beta = \frac{4\pi D}{\int_r^\infty \frac{e^{(\frac{\psi(r)}{kT})}}{r^2} dr} \qquad \psi(r) = -\frac{q^2 P_0}{er^2}$$

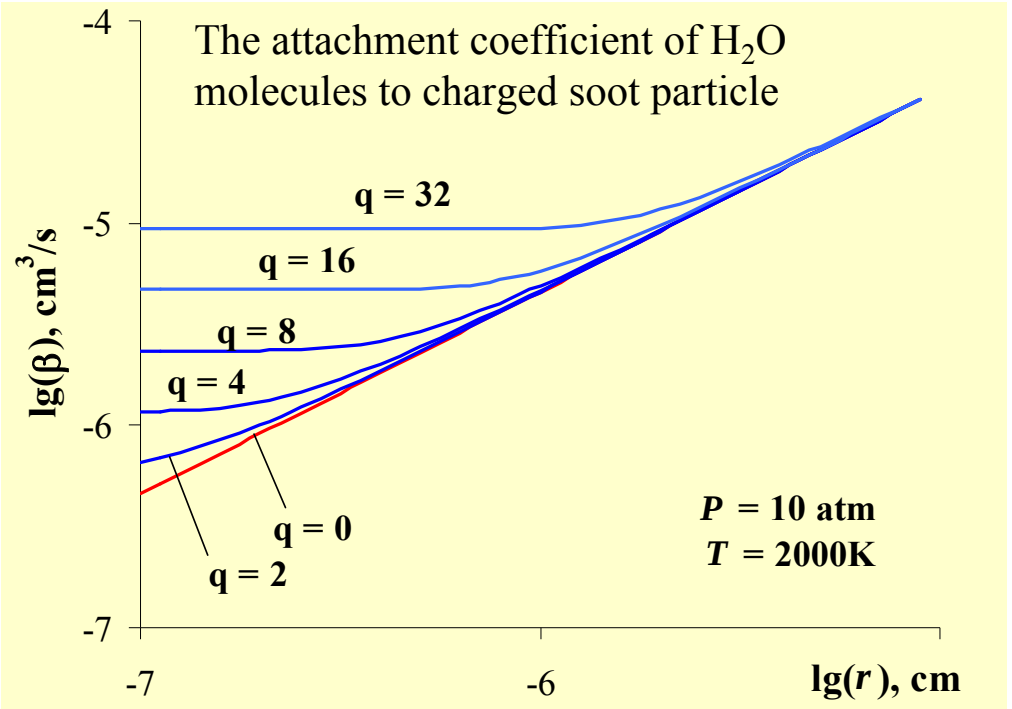

- **For charged soot particles the attachment coefficient of polar molecules is considerably greater (in a factor of 10-20) than that for neutral ones.**
- **For typical value of soot particle concentration N_S=10^7 cm^{-3} the deposition time for H_2O molecule to charged soot particle is ~ 10 ms.**
- **Acquisition of polar molecules by soot particles makes it possible to deposit the water soluble materials on the particle surface directly inside the combustor, as a result, a primary hydrophobic soot particles become hydrophilic.**

- **Charged soot particles may be activated as cloud condensation nuclei directly inside the combustor**

Interaction of charged particles with dipole molecules

Interaction potential under supposition of equilibrium distribution of dipole momentum vector orientation of polar molecules in presence of a point charge.

$$\Phi_{pd}(r) = -\frac{pze}{4\pi\varepsilon_0 r^2} L\left(\frac{pze}{4\pi\varepsilon_0 r^2 k_B T}\right)$$

r – distance from a molecule to a point charge,
z – particle charge in elementary charge units,
p – inherent dipole moment of a molecule,
ε_0 – electric constant, e – electron charge,
α– mean molecular polarizability,
L - Lagrange function.

Interaction cross-section of particle and polar molecule.

$$\sigma(E) = \pi R^2 \left(1 - \Phi_{pd}(R)/E_0\right)$$

E_0 – full energy of relative motion of polar molecule in the infinity

Rate constant of polar molecule attachment to a particle under supposition, that interaction potential corresponds to a central force field.

$$K_{pd} = \pi R_0^2 \sqrt{\frac{8k_B T}{\pi\mu_{pd}}} \left\{ y \frac{e^{-y} + e^{y}}{e^{-y} - e^{y}} \right\},\ y = \frac{pe}{4\pi\varepsilon_0 R_0^2 k_B T}$$

Supposition of equilibrium distribution of polar molecule over the orientation of dipole moment vector is valid only for the case of high pressure, when many collisions occur in the vicinity of a particle, and an equilibrium distribution is established as a result. In this case Kn_p=1, i.e. diffusion regime, when attachment rate is limited by diffusion of polar molecules towards particle.

In our case Kn_p>>1, there are no collisions in the vicinity of a particle, and there are no reasons to suppose that the interaction potential is described by the above formula.

Properties of soot particles emitted from aeroengine

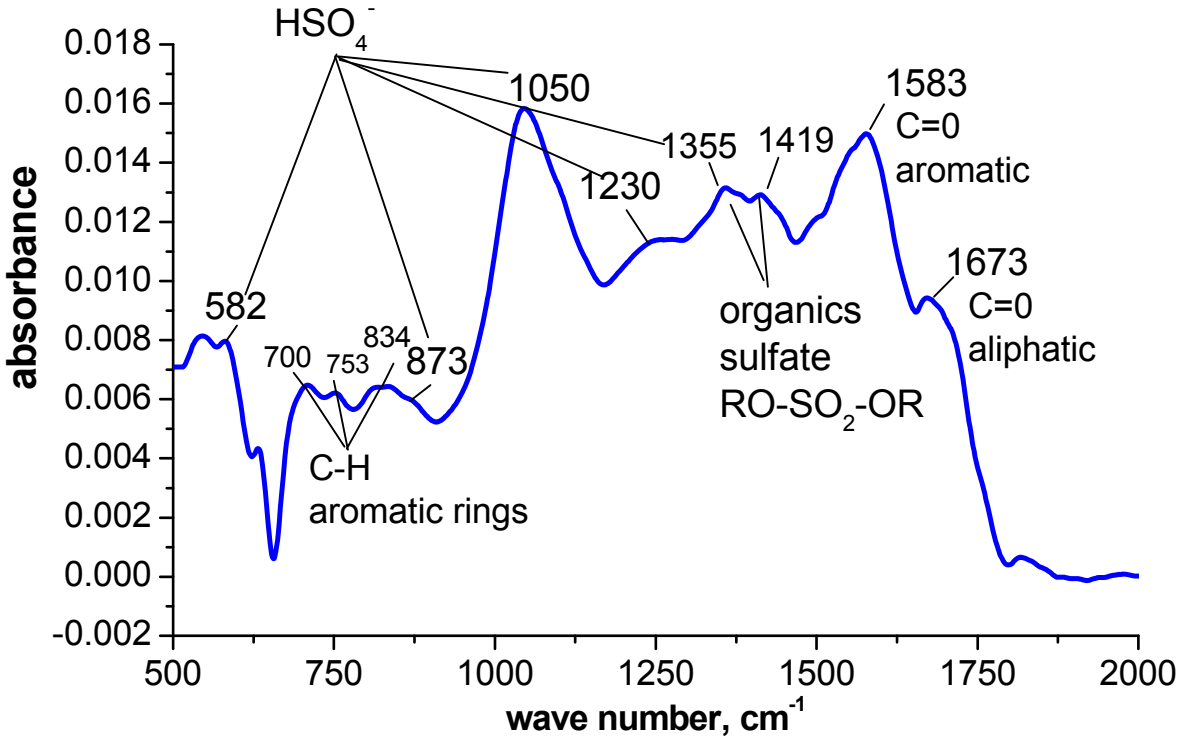

The soot sample has been collected behind the aero-engine combustor operating at cruise. To study the chemical nature of the soot surface the Fourier Transform Infrared Spectroscopy has been used (*Popovicheva et al., Geophys. Res. Lett, 2004*).

Two types of soot were observed in the sample:

✓ the first type consists mainly of amorphous black carbon (hydrophobic fraction),

✓ the second one contains different impurities (ionic sulfate, organic sulfate) on the soot particle surface (hydrophilic fraction), this fraction has 13%wt of water soluble material on its surface

Properties of soot particles emitted from aeroengine

Combustor soot was collected at the exit plane of aviation combustor. Soot *TC1* was collected above the flame upon the burning the same aviation kerosene with FSC=0.1%

Combustor soot is more hydrophilic than the soot produced in flame

Amount of adsorbed water molecules per unit of surface for TC1 and combustor soot at T=295K.

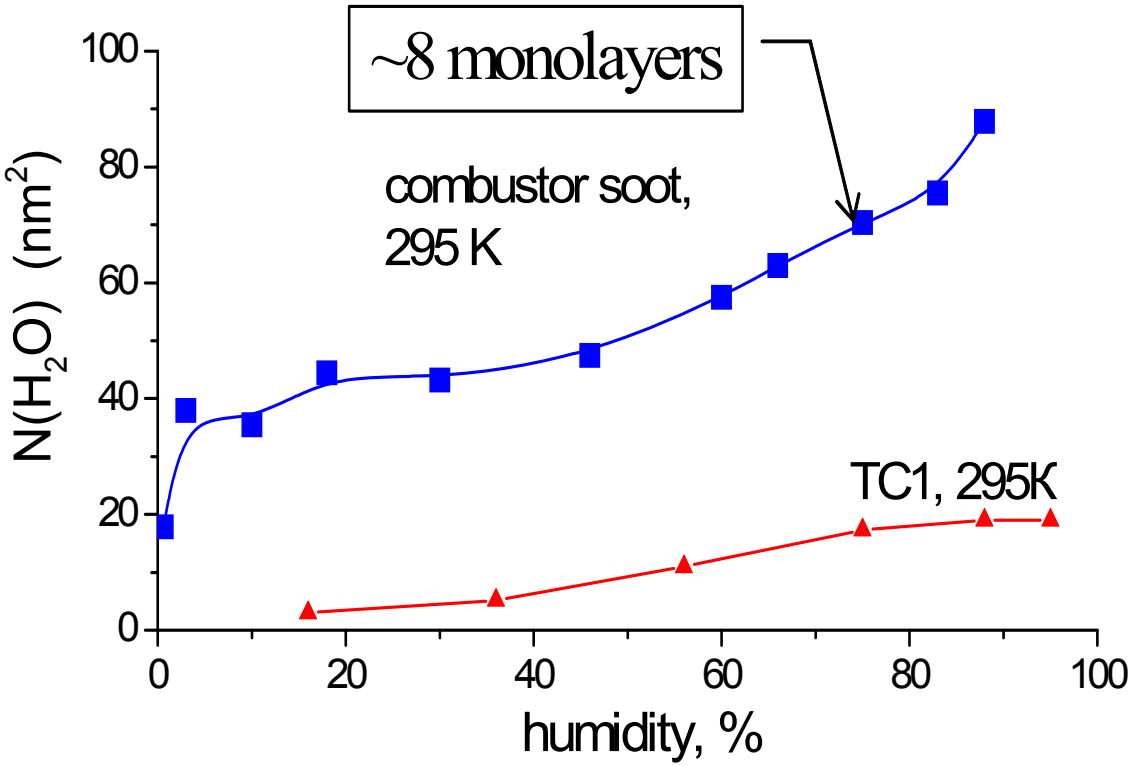

Possible reason to gain the hydrophilic properties by combustor soot is supposed to be following :
Deposition of polar molecules (H_2O, H_2SO_4, organics and others) on the surface of small charged particles and on the primary clusters during the soot formation in the fuel enriched region of combustor.

Combustion of metallized and composite fuels comprising energetic nanocomponents

Energetic properties of different fuels

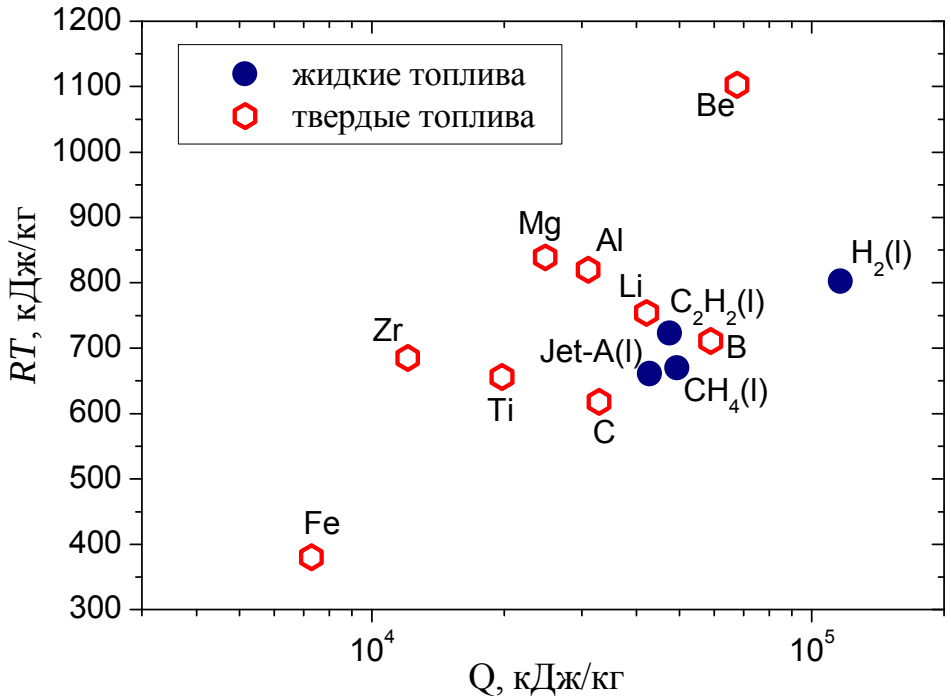

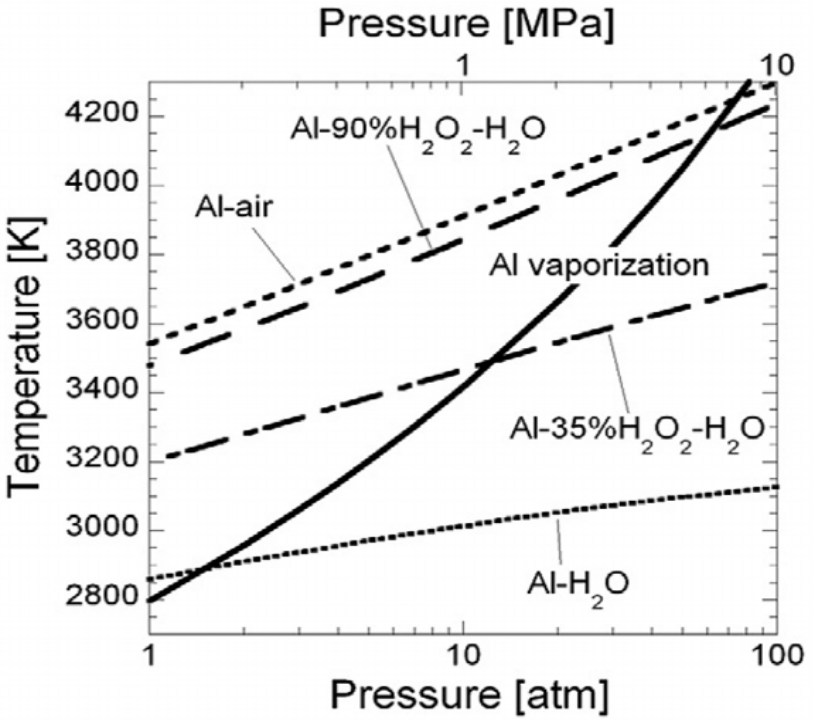

Fig. 1. Comparison of various adiabatic flame temperatures of stoichiometric Al combustion systems with Al vaporization temperatures over a range of pressure.

Composite fuels: C_nH_m+ nano-Al

It is needed to develop novel kinetic models involving

- **processes in gas phase,**
- **formation of condensed phase,**
- **formation of ions, electrons and charged clusters,**
- **formation of ecologically harmful species**

For such fuels, the additional ions form: Al^+, AlO^+, $AlOH^+$ and others

We are at the starting stage!

Combustion of composite fuels comprising hydrocarbons and Al nanoparticles

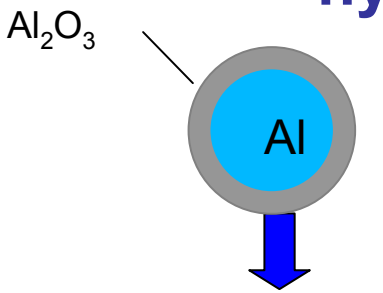

The time of heating the Al particle with r =10 nm due to thermal conductivity

τ_h~1 ps.

The time of oxide layer formation

τ_{ox}~100 ps.

Gasification of particles with r < 25 nm (this is confirmed by the shock tube experiments: Al atoms were recorded and MD calculations). Melt dispersion mechanism was proposed by Levitas C&F 2009, 2014

Kinetic models: Al-O_2 -*Swihart et al., C&F 2000*; Al-O_2-H_2O - Huang et al. *C&F 2009; Washburn et al. C&F 2008: Starik et al . C&F 2014; Al-CH_4-O_2*(air) - *Starik et al . Energy&Fuel 2014.*

Gas phase kinetic model of hydrocarbon(CH_4)-Al-air and Al-H_2O mixtures oxidation:

1. The reaction mechanism of Al oxidation was built (60 reactions, 24 species):
   - reaction channels were determined (*ab initio* method)
   - rate constants were calculated
2. Thermodynamic properties (H, S, ΔG) for Al-containing species were determined:
   - rotational constants, vibrational frequencies, statistical weight, symmetry number for Al-containing species were calculated
3. Transport coefficients (D_{ij}, λ_i) were determined **by using**
   - dipole moments, tensors of polarizability, Van-der-Waals molecule radii calculated on the base of quantum chemistry methods

[Sharipov, Titova, Starik, Combustion Theory and Modelling, 2012]

Unresolved problems

- There is little information on kinetic data needed to built the detailed reaction mechanism in Al/C/H/O/N system to simulate the ignition and combustion of metalized and composite fuels comprising Al particles with formation of condensed phase

- What is the structure of stable ionic clusters forming in the combustion exhaust?

- What kind of charge and neutral particles can form during combustion of metallized and composite fuels

I am grateful to the co-workers of my Research Center “Physics of Non-equilibrium Processes and Novel Combustion Concepts”

Many thanks for your attention